

OTFS: Interleaved OFDM with Block CP

Vivek Rangamgari*, Shashank Tiwari*, Suvra Sekhar Das*, and Subhas Chandra Mondal†
*G.S Sanyal School of Telecommunication, Indian Institute of Technology, Kharagapur, India
† Wipro Limited, Bangalore, India

Abstract—Orthogonal time frequency space (OTFS) modulation is a recently proposed waveform for reliable communication in high-speed vehicular communications. It has better resilience to inter-carrier interference (ICI) as compared to orthogonal frequency division multiplexing (OFDM). In OTFS, information is generated in the Doppler-delay domain as opposed to time-frequency domain in conventional OFDM. In this work, we describe OTFS as block-OFDM with a cyclic prefix and time interleaving. Through this description, we explained the improved performance of OTFS over OFDM. We also compare the performance of OTFS against its contender 5G new radio (NR)’s OFDM configuration of variable subcarrier bandwidth (VSB) while considering practical forward error correction codes and 3GPP high-speed channel model. We have considered practical channel estimates in the demodulation and find that OTFS outperforms VSB with 5G NR parameter. We also study the influence of pilot in OTFS in its peak to average power ratio (PAPR).

Index Terms—OFDM, OTFS, 5G NR, ASB, Doppler, ICI, phase noise, time-varying channel

I. INTRODUCTION

With 5G, there is a growing demand for providing good quality of service in high speed vehicular scenarios [1] such as in vehicular to vehicular communications (V2V), unmanned aerial vehicle (UAV) communications, etc. Orthogonal Frequency Division Multiplexing (OFDM), which has found its place in many wireless communications technologies is limited in providing reliable connection in high speed vehicular scenarios due to its high sensitivity to inter carrier interference (ICI), which is attributed to Doppler spread and phase noise. Recently, Orthogonal Time Frequency Space (OTFS) modulation proposed in [2] is shown to be superior to OFDM in such high mobility environments.

In OTFS, the user data is placed in the delay-Doppler (De-Do) domain as opposed to time-frequency grid in OFDM. The data is then spread across the time-frequency grid using a unitary transform which opens up opportunity to extract diversity gain. This is followed by an OFDM [2] or block OFDM [3] modulator and a cyclic prefix (CP) [2] or block CP [3] is added to absorb the channel delay spread. When OFDM modulation is used with CP ; such variant of OTFS can be termed as CP-OTFS [2]. Whereas, OTFS with block OFDM modulation and block CP is termed as reduced CP OTFS (RCP-OTFS) [4]. The latter has better spectral efficiency than CP-OTFS. In this paper, we consider the the second one i.e. RCP-OTFS. Advanced receivers are required to extract diversity gain as OTFS suffers from ISI and ICI when exposed to a time variant channel [5]. There can be two types of receivers namely (i) Linear receivers such as in [6] and (ii) Non-linear receivers

such as in [7] which can extract the diversity gain. Non-linear receivers have better BER performance as opposed to linear receivers at the cost of higher computational complexity. We limit this study to linear receiver.

In this paper, we exploit the matrix factorization of OTFS modulation matrix to show that OTFS can also be interpreted as a block-OFDM with a single cyclic prefix and time interleaving where samples from all the OFDM symbols are interleaved in time which simplifies the way we understand OTFS signal generation. Thus the primary difference between OTFS and block OFDM can be viewed as time interleaving of block OFDM samples, which provides an opportunity for diversity gain in OTFS. It is known that error correction codes also extracts diversity gain. The question arises what is the cumulative diversity gain achievable when (i) spreading in time-frequency (ii) interleaving in time domain and (iii) FEC is used as compared to OFDM with FEC.

It is known for quite some time now that variable subcarrier bandwidth OFDM (VSB-OFDM) [8] [9] [10] can be used to improve the resilience of OFDM to ICI, a variant of which is adopted in 5G NR [11], where VSB reconfigurability is expressed in terms of ‘numerology’. Since such VSB schemes are part of already standardized 5G whereas OTFS claim to improve upon 5G NR, we aim to evaluate the performance of VSB-OFDM against OTFS in realistic channel profile namely 3GPP as specified in [12] with LDPC codes and practical channel estimation, in this work.

Previous works have shown coded performance comparison between CP-OTFS with OFDM [13] and with VSB-OFDM [5]. Moreover uncoded performance of RCP-OTFS is compared with OFDM in [7]. To the best of author’s knowledge, coded performance of RCP-OTFS is not compared with VSB-OFDM along with practical channel estimation under practical vehicular channel model. To the best of author’s knowledge, there is a limited literature available which evaluate interleaving gain of OTFS over block OFDM system.

As mentioned above, we consider practical channel estimation. We also look into pilot power aspect, as it may have impact on peak to power ratio (PAPR) of OTFS signal since the pilot signal in OTFS is an impulse in De-Do domain.

We follow the notations described below throughout the paper. We use \mathbf{Z} , \mathbf{z} , z as Matrix, Vector and scalar respectively. $()^T$ and $()^\dagger$ denote transpose and hermitian operations. W_L and I_N represents L order normalized Inverse Discrete Fourier Transform (IDFT) matrix and N order Identity matrix. Kronecker product operator is given by \otimes . The operator $\text{diag}\{\mathbf{x}\}$ creates a diagonal matrix with the elements of

vector \mathbf{x} . Circulant matrix is represented by $\text{circ}\{\mathbf{x}\}$ whose first column is \mathbf{x} . Notations $\lfloor - \rfloor$ and $\lceil - \rceil$ are floor and ceil operators respectively. Column-wise vectorization of matrix (\mathbf{X}) is represented by $\text{vec}\{\mathbf{X}\}$. Natural numbers are denoted by \mathbb{N} whereas $j = \sqrt{-1}$.

II. RCP-OTFS

A. OTFS Transmission

We consider RCP-OTFS system operating with time-frequency resource of total T_f sec. duration and B Hz. The Bandwidth is divided into M number of sub-carriers having Δf sub-carrier bandwidth and we transmit N number of symbols having T symbol duration, thus $B = M\Delta f$ and $T_f = NT$. Furthermore, OTFS is critically sampled, i.e $T\Delta f = 1$

The source bitstream is encoded using LDPC codes and then passed through symbol mapper. The QAM modulated Doppler-delay data and pilot symbols are arranged over Doppler-delay lattice $\Lambda = \{(\frac{k}{NT}, \frac{l}{M\Delta f})\}$, $k \in \mathbb{N}[0 N - 1]$, $l \in \mathbb{N}[0 M - 1]$ as shown in Fig.2a. Doppler-delay signal can be given as,

$$x(k, l) = \begin{cases} x_p, & k = K_p \ \& \ l = L_p \\ 0 & K_p - 2k_\nu \leq k \leq K_p + 2k_\nu \ \& \\ & L_p - 2l_\tau \leq l \leq L_p + 2l_\tau \\ d(k, l), & \text{otherwise} \end{cases} \quad (1)$$

where $d(k, l) \in \mathbb{C}$ is the QAM data symbol, $x_p = \text{sqr}(P_{\text{pilot}})$ is the pilot symbol, P_{pilot} is power of pilot symbol, $k_\nu = \lceil \nu_{\text{max}} NT \rceil$ and $l_\tau = \lceil \tau_{\text{max}} M \Delta f \rceil$ are maximum doppler length and delay length of the channel [14] and (K_p, L_p) is the pilot location, $K_p \in \mathbb{N}[2k_\nu + 1 N - 2k_\nu - 2]$, $L_p \in \mathbb{N}[l_\tau + 1 M - l_\tau - 2]$.

Then, $x(k, l)$ is mapped to time-frequency data $Z(n, m)$ on lattice $\Lambda^\perp = \{(nT, m\Delta f)\}$, $n \in \mathbb{N}[0 N - 1]$ and $m \in \mathbb{N}[0 M - 1]$ by using inverse symplectic finite Fourier transform (ISFFT). Thus $Z(n, m)$ can be given as,

$$Z(n, m) = \frac{1}{\sqrt{NM}} \sum_{k=0}^{N-1} \sum_{l=0}^{M-1} x(k, l) e^{j2\pi[\frac{nk}{N} - \frac{ml}{M}]}. \quad (2)$$

The time domain signal is obtained from $Z(n, m)$ using Heisenberg transform as,

$$s(t) = \sum_{n=0}^{N-1} \sum_{m=0}^{M-1} Z(n, m) g(t - nT) e^{j2\pi m \Delta f (t - nT)} \quad (3)$$

where, $g(t)$ is transmitter pulse of duration T . In this paper, we consider $g(t)$ to be a rectangular pulse as in [4], i.e,

$$g(t) = \begin{cases} 1 & 0 \leq t \leq T \\ 0 & \text{otherwise} \end{cases} \quad (4)$$

To obtain discrete version of OTFS system, $s(t)$ is sampled at the sampling interval of $\frac{T}{M}$ and $\mathbf{s} = [s(0) s(1) \dots s(MN - 1)]$ is formed from the samples of $s(t)$.

The Doppler-delay symbols $x(k, l)$ are arranged in $M \times N$ matrix as,

$$\mathbf{X} = \begin{bmatrix} x(0, 0) & x(0, 1) & \dots & x(0, N - 1) \\ x(1, 0) & x(1, 1) & \dots & x(1, N - 1) \\ \vdots & \vdots & \ddots & \vdots \\ x(M - 1, 0) & x(M - 1, 1) & \dots & x(M - 1, N - 1) \end{bmatrix} \quad (5)$$

The time domain signal can also be written as matrix-vector multiplication,

$$\mathbf{s} = \mathbf{A} \mathbf{x} \quad (6)$$

where, $\mathbf{x} = \text{vec}\{\mathbf{X}\}$ and $\mathbf{A} = \mathbf{W}_N \otimes \mathbf{I}_M$ denotes the OTFS transform ISFFT matrix. A cyclic prefix (CP) of length $L \geq l_\tau$ is appended at the start of the \mathbf{s} .

B. OTFS as interleaved Block OFDM

The time-frequency signal obtained in (2) can be expressed in matrix form \mathbf{Z} as,

$$\mathbf{Z} = \mathbf{W}_M^\dagger \mathbf{X} \mathbf{W}_N \quad (7)$$

The OTFS time domain signal \mathbf{s} is obtained by applying IDFT along the frequency axis and given as,

$$\mathbf{s} = \text{vec}\{\mathbf{W}_M \mathbf{Z}\} \quad (8)$$

which is simplified as,

$$\mathbf{s} = \text{vec}\{\mathbf{X} \mathbf{W}_N\} \quad (9)$$

If Block OFDM is used to transmit the same data assuming \mathbf{X} in time-frequency domain with N subcarriers and M OFDM symbols, then the time domain signal can be expressed as,

$$\mathbf{s}_{\text{bofdm}} = \text{vec}\{\mathbf{W}_N \mathbf{X}^T\} \quad (10)$$

From (9) and (10),

$$\mathbf{s}(nM + m) = \mathbf{s}_{\text{bofdm}}(mN + n) \quad (11)$$

where $m \in \mathbb{N}[0 M - 1]$ and $n \in \mathbb{N}[0 N - 1]$.

Therefore it can be said that OTFS transmitted signal \mathbf{s} can be obtained by shuffling block OFDM transmitted signal $\mathbf{s}_{\text{bofdm}}$ using the simple relationship (11). Thus, it is established that OTFS can be seen as block OFDM with time interleaving. Moreover, it must be noted that parameters for OTFS and its equivalent Block OFDM system is different. For the same time-frequency resource of T_f sec and B Hz, OTFS system has M subcarriers and N OTFS symbols whereas equivalent Block OFDM system has $M_{\text{bofdm}} = N$ subcarriers and $N_{\text{bofdm}} = M$ OFDM symbols. Therefore, the subcarrier bandwidth for the equivalent Block OFDM system changes to $\Delta f_{\text{bofdm}} = \frac{M}{N} \Delta f$ and OFDM symbol duration changes to $T_{\text{bofdm}} = \frac{N}{M} T$. In general $M > N$, thus $\Delta f_{\text{bofdm}} > \Delta f$ which implies that OTFS will have increased capability to combat Doppler as opposed to an OFDM system having Δf sub-carrier bandwidth. Fig. 1 shows the time domain signal generation for different waveforms and depicts the RCP-OTFS as block OFDM with time interleaving.

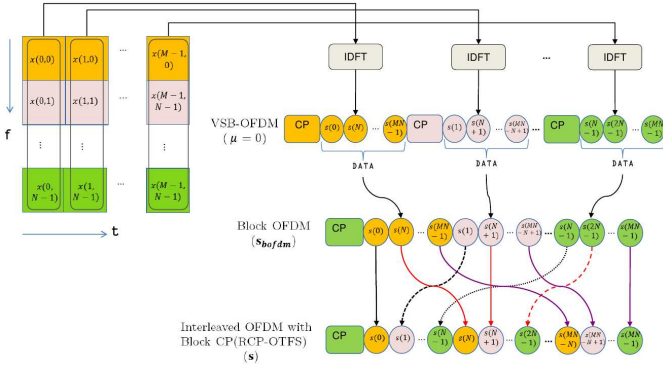


Fig. 1: Time domain signal construction in CP-OFDM, Block OFDM and RCP-OTFS

C. Channel

We consider a time varying channel of P paths with h_p complex attenuation, τ_p delay and ν_p Doppler value for p th path where $p \in [1 P]$. Thus, delay-Doppler channel spreading function can be given as,

$$h(\tau, \nu) = \sum_{p=1}^P h_p \delta(\tau - \tau_p) \delta(\nu - \nu_p) \quad (12)$$

The delay and Doppler values for p th path is given as $\tau_p = \frac{l_p}{M\Delta f}$ and $\nu_p = \frac{k_p}{NT}$ where $l_p \in \mathbb{N}[0 M - 1]$ and $k_p \in \mathbb{N}[0 N - 1]$ are delay and Doppler bin number on Doppler-delay lattice Λ for p^{th} path. We assume that N and M are sufficiently large so that there is no effect of fractional delay and Doppler on the performance.

We also define time varying frequency response of channel $h_{tf}(t, f)$ as,

$$h_{tf}(f, t) = \int_0^{\tau_{\max}} \int_0^{\nu_{\max}} h(\tau, \nu) e^{j2\pi(\nu t - f\tau)} d\nu d\tau \quad (13)$$

which simplifies as,

$$h_{tf}(f, t) = \sum_{p=1}^P h_p e^{j2\pi(\nu_p t - f\tau_p)} \quad (14)$$

Its discrete version $\hat{h}(m, n)$, the channel coefficient at m th subcarrier of n th time symbol used later in III-B, is defined as,

$$\hat{h}(m, n) = h_{tf}(f, t) \Big|_{f=m\Delta f, t=nT} \quad (15)$$

D. Receiver

After removal of CP at the receiver, the received signal can be written as [6],

$$\mathbf{r} = \mathbf{H}\mathbf{s} + \mathbf{n} \quad (16)$$

where, \mathbf{n} is white Gaussian noise vector of length MN with elemental variance σ_n^2 and \mathbf{H} is a $MN \times MN$ channel matrix and can be given as,

$$\mathbf{H} = \sum_{p=1}^P h_p \mathbf{\Pi}^{l_p} \mathbf{\Delta}^{k_p} \quad (17)$$

with $\mathbf{\Pi} = \text{circ}\{[0 \ 1 \ 0 \ \dots \ 0]^T\}_{MN \times MN}$ is a circulant delay matrix and $\mathbf{\Delta} = \text{diag}\{[1 \ e^{j2\pi \frac{1}{MN}} \ \dots \ e^{j2\pi \frac{MN-1}{MN}}]^T\}$ is a diagonal Doppler matrix.

a) *Channel Estimation*: Channel matrix \mathbf{H} is estimated from the pilot symbols. The received signal is transformed to Doppler-delay domain as,

$$\mathbf{y} = \mathbf{A}^\dagger \mathbf{r} \quad (18)$$

The Doppler-delay received vector \mathbf{y} is reshaped back to the $N \times M$ grid as

$$\mathbf{Y}(k, l) = \mathbf{y}(k + lN) \quad (19)$$

where $k \in \mathbb{N}[0 N - 1]$, $l \in \mathbb{N}[0 M - 1]$. The channel estimation from here proceeds according to [15], in which the non zero pilot at location (K_p, L_p) as shown in fig.2a is spread to locations (k, l) , $k \in \mathbb{N}[K_p - k_\nu \ K_p + k_\nu]$ and $l \in \mathbb{N}[L_p \ L_p + l_\tau]$ because of the channel.

The channel parameters (h_p, k_p, l_p) are extracted from this region using the threshold based scheme with threshold (Υ) as $3\sigma_n$ given as,

$$(\hat{h}_p, \hat{k}_p, \hat{l}_p) = (Y(k, l), k, l)$$

$\ni \|Y(k, l)\| > \Upsilon \ \forall \ K_p - k_\nu \leq k \leq K_p + k_\nu \ \& \ L_p \leq l \leq L_p + l_\tau$

From the channel parameters, the channel matrix \mathbf{H} is formed as,

$$\hat{\mathbf{H}} = \sum_{p=1}^{\hat{P}} \hat{h}_p \mathbf{\Pi}^{\hat{l}_p} \mathbf{\Delta}^{\hat{k}_p}$$

where \hat{P} is the number of taps detected.

b) *Equalization*: The Doppler-delay data is estimated by equalizing the received time domain signal using MMSE [6] as,

$$\hat{\mathbf{x}} = \mathbf{H}_{\text{mmse}} \mathbf{r} \quad (20)$$

where

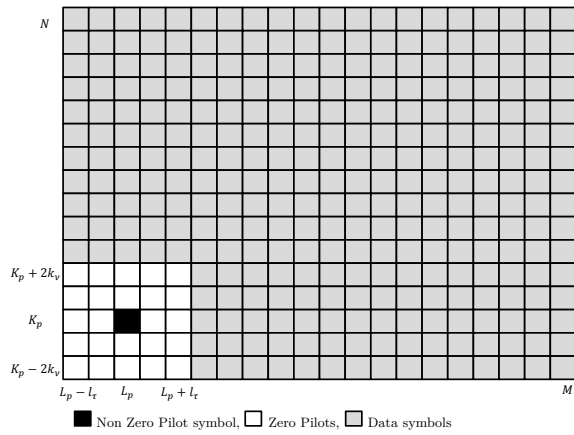
$$\mathbf{H}_{\text{mmse}} = (\hat{\mathbf{H}}\mathbf{A})^\dagger [(\hat{\mathbf{H}}\mathbf{A})(\hat{\mathbf{H}}\mathbf{A})^\dagger + \frac{1}{\Gamma}\mathbf{I}]^{-1}$$

To decode the equalized data using LDPC decoder, the log-likelihood ratios (LLRs) are passed to the decoder which are calculated from the equalized symbols as,

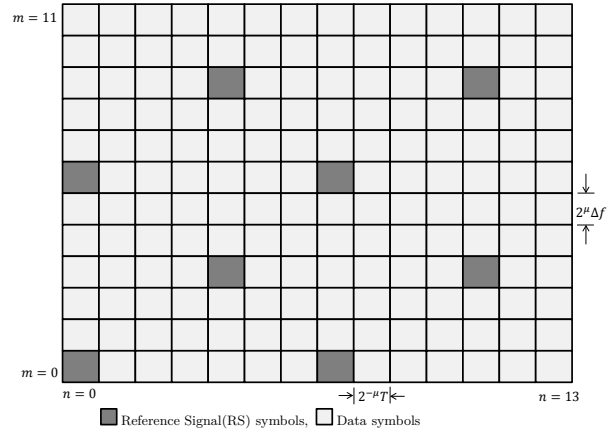
$$LLR(b_\eta^j | \hat{x}(\eta)) \approx \left(\min_{s \in S_j^0} \frac{|\hat{x}(\eta) - s|^2}{\sigma^2(\eta, \eta)} \right) - \left(\min_{s \in S_j^1} \frac{|\hat{x}(\eta) - s|^2}{\sigma^2(\eta, \eta)} \right) \quad (21)$$

where $\hat{x}(\eta)$ is the η^{th} element of $\hat{\mathbf{x}}$ mapped from the bits $b_\eta^0 \ b_\eta^1 \ \dots \ b_\eta^{K-1}$, K is the number of bits per symbol and $\sigma^2(\eta, \eta)$ is the element of $\sigma^2 = \sigma_n^2 (\mathbf{H}_{\text{mmse}} \mathbf{H}_{\text{mmse}}^\dagger)$. S_j^0 and S_j^1 denotes the set of constellation symbols where the bit $b_\eta^j = 0$ and $b_\eta^j = 1$ respectively for $j = 0, 1, \dots, K - 1$.

These LLRs are then fed into the LDPC decoder to decode data. Let \mathbf{L} denotes a matrix where $\mathbf{L}(\eta, j) = LLR(b_\eta^j | \hat{x}(\eta))$ for $\eta = 1, 2, \dots, MN$ and $j = 0, 1, \dots, K - 1$. \mathbf{L} is reshaped to $L_{cl} \times N_{cw}$ matrix where L_{cl} and N_{cw} denote the LDPC codeword length and number of codewords respectively. Each



(a) RCP-OTFS



(b) VSB-OFDM

Fig. 2: Pilot placement in RCP-OTFS and in a PRB of VSB-OFDM

column of \mathbf{L} subsequently regenerates message word m_ℓ for $\ell = 1, 2, \dots, N_{cw}$ using the Min-Sum algorithm [16] employed by the LDPC decoder and is collected as the recovered data.

III. VSB OFDM OVERVIEW

We consider a VSB-OFDM system with total frame duration T_f sec. and bandwidth B Hz. We have a base sub-carrier bandwidth of Δf Hz and variability in the sub-carrier bandwidth is introduced by the parameter μ . For a given μ , the subcarrier bandwidth is $2^\mu \Delta f$ Hz. We have total $2^{-\mu} M$ number of sub-carriers and $2^\mu N$ number of OFDM symbols having $2^{-\mu} T$ symbol duration, thus $B = M \Delta f$ and $T_f = NT$.

A. Transmitter

We use the Physical Resource Block (PRB) Frame structure of 5G NR for VSB-OFDM system. Each PRB consists of 12 subcarriers \times 14 time slots with 8 reference signals (RS) as shown in Fig.2b. Then the PRBs are arranged to fill the time-frequency grid of B Hz and T_f sec. The number of PRBs in a given frame is,

$$N_{PRB} = \left\lfloor \frac{B}{12 \cdot 2^\mu \cdot \Delta f} \right\rfloor \left\lfloor \frac{T_f}{14 \cdot 2^{-\mu} \cdot T} \right\rfloor$$

The source bits are encoded using LDPC code and then passed through the symbol mapper. The modulated QAM symbols are arranged in the N_{PRB} number of PRBs to form the time-frequency signal $\hat{x}(m, n)$, $m \in \mathbb{N}[0 \ 2^{-\mu} M - 1]$ and $n \in \mathbb{N}[0 \ 2^\mu N - 1]$ in a frame. Then, the n th time domain OFDM symbol can be given as,

$$\hat{s}_n(t) = \sum_{m=0}^{2^{-\mu} M - 1} \hat{x}(m, n) e^{j2\pi m 2^\mu \Delta f (t - n 2^{-\mu} T)} \quad (22)$$

where $2^{-\mu} T$ is the one OFDM symbol duration without CP. Further, if $\hat{\mathbf{x}}_n$ represents the discrete version of $\hat{s}_n(t)$ sampled

at $\frac{1}{B}$, then the $2^\mu N$ concatenated OFDM symbols can be given as,

$$[\hat{\mathbf{x}}_0 \ \hat{\mathbf{x}}_1 \ \dots \ \hat{\mathbf{x}}_{2^\mu N}] = \mathbf{W}_{2^{-\mu} M} \hat{\mathbf{X}} \quad (23)$$

where $\hat{\mathbf{X}}$ is the time-frequency frame given as,

$$\hat{\mathbf{X}} = \begin{bmatrix} \hat{x}(0, 0) & \dots & \hat{x}(0, 2^\mu N - 1) \\ \hat{x}(1, 0) & \dots & \hat{x}(1, 2^\mu N - 1) \\ \vdots & \ddots & \vdots \\ \hat{x}(2^{-\mu} M - 1, 0) & \dots & \hat{x}(2^{-\mu} M - 1, 2^\mu N - 1) \end{bmatrix}$$

Then, Cyclic Prefix (CP) is appended to each OFDM symbol of duration $2^{-\mu} T_{cp}$ sec such that $T_o = T + T_{cp}$

B. Receiver

Assuming the CP duration is greater than maximum excess delay of channel, one OFDM symbol duration is within a coherence time and subcarrier bandwidth within coherence bandwidth. Then after removing CP and taking the DFT, the received time-frequency symbol $\hat{y}(m, n)$ can be expressed as,

$$\hat{y}(m, n) = \hat{h}(m, n) \hat{x}(m, n) + \hat{v}(m, n) \quad (24)$$

where, $m \in \mathbb{N}[0 \ 2^{-\mu} M - 1]$ is the subcarrier index and $n \in \mathbb{N}[0 \ 2^\mu N - 1]$ is the OFDM symbol index. $\hat{h}(m, n) \in \mathbb{C}$ defined in (15) is the channel coefficient and $\hat{v}(m, n) \in \mathbb{C}$ is white gaussian noise with variance σ_V^2 at m th subcarrier of n th OFDM symbol.

For channel estimation, the Reference signal symbols in the a PRB is used to get the estimates at the pilot location using MMSE estimation as,

$$\hat{h}(m_{RS}, n_{RS}) = \frac{\hat{x}(m_{RS}, n_{RS})^\dagger \hat{y}(m_{RS}, n_{RS})}{\|\hat{x}(m_{RS}, n_{RS})\|^2 + \sigma_V^2} \quad (25)$$

where $(m_{RS}, n_{RS}) = \{(0, 0), (6, 0), (3, 4), (9, 4), (0, 7), (6, 7), (3, 11), (9, 11)\}$ are the position of RS in a PRB.

The obtained channel estimates at the RS locations in time-frequency grid are interpolated to get the channel estimates

at the data locations using DFT interpolation along frequency axis and linear interpolation along time axis as in [17].

The estimate of data symbols are obtained at the receiver using,

$$\hat{x}(m, n) = \frac{\hat{y}(k, l)}{\hat{h}(k, l)} \quad (26)$$

The estimated symbols are used to generate the channel LLR values of bits corresponding to the symbol by substituting $\sigma^2 = \text{diag}\{\text{vec}\{\sigma_{\mathbf{V}_{\text{eff}}}^2\}\}$ in (21) where $\sigma_{\mathbf{V}_{\text{eff}}}^2(m, n) = \frac{\sigma_v^2}{\|\hat{h}(m, n)\|^2}$. Then LLRs are used to recover the data as described in II-D.

IV. PILOT POWER IN OTFS AND VSB-OFDM

Pilots are needed for channel estimation in all transmission schemes. In this section we describe the pilot structure to be used in OTFS as in [15]. We also describe the pilot structure used for evaluating VSB-OFDM. In the performance evaluation, we intend to keep same total transmit power for OTFS and OFDM. As shown in Fig.2b, there are 8 pilots per PRB in VSB-OFDM system considered. The total number of pilots in VSB-OFDM frame is $N_{p,ofdm} = 8N_{PRB}$, while total number of pilots in RCP-OTFS is $N_{p,otfs} = (4k_\nu + 1)(2l_\tau + 1) - 1$ [15]. If we let the total pilot power to be equal, i.e $P_{pilot} = n_{p,ofdm}P_T = n_{p,otfs}P_T$ where P_T is the transmit power, $n_{p,otfs}$ and $n_{p,ofdm}$ are the ratio of number of pilot symbols to total number of symbols for RCP-OTFS and VSB-OFDM respectively. Since, RCP-OTFS uses only one non-zero pilot at location (K_p, L_p) and $(N_{p,otfs} - 1)$ zero pilots as shown in Fig.2a, total pilot power is placed on the pilot symbol (x_p) which results in an uneven power distribution for pilots and data in RCP-OTFS given by $\Delta P = 10\log_{10}(\frac{P_{pilot}}{P_{data}})$. Value of ΔP is 34 dB for the RCP-OTFS system, for parameters given in Table I. If P_T is to be kept same as VSB-OTFS system. We evaluate the impact of ΔP on PAPR in Sec.V below.

V. RESULTS

TABLE I: Simulation Parameters

Parameter	Value
Carrier Frequency(f_c)	6 GHz
Bandwidth(B)	7.68 MHz
Frame Time(T_f)	10 ms
Subcarrier Bandwidth(Δf)	15 KHz
RCP-OTFS parameters	M=512, N=128, $K_p=80$, $L_p=16$
VSB-OFDM parameters	M=512, N=128, $\mu=0,1,2,3$
Equivalent OFDM parameters	$M_{bofdm}=128$, $N_{bofdm}=512$, $\Delta f_{bofdm} = 60$ KHz
Channel Model [12]	TDL-A, DS=37 ns, Rural Macro
CP duration(T_{cp})	4.69 μ s
UE speed	500 kmph
FEC	QC-LDPC, coderate 2/3, Codeword Length 1944

In this section, We present the LDPC coded performance of OTFS, block OFDM and VSB-OFDM system. The simulation parameters are mentioned in Table I. The key performance indicator (KPI) used to evaluate performance is block error

rate (BLER), where block is a coded block of LDPC code, which is 1944 bits in this work. For block OFDM system, we consider same frame size as RCP-OTFS. Time-frequency slots for block OFDM can be evaluated as described in Sec.II-B as $M_{bofdm} = 128$, $N_{bofdm} = 512$, and $\Delta f_{bofdm} = 60$ KHz. It may be noted that we use the same LMMSE based interference cancellation equalizer for RCP-OTFS and block OFDM so that any difference in BLER performance can be attributed to interleaving only. The SNR due to CP, which is given as $10\log_{10}(\frac{[T_{cp}B]}{M}) = 0.3$ dB for VSB-OFDM and $10\log_{10}(\frac{[T_{cp}B]}{MN}) = 0.0023$ dB for OTFS is also adjusted in the results. Moreover, same transmit power is ensured for all the transmission schemes. Doppler is generated using Jake's formula, $\nu_p = \nu_{max} \cos(\theta_p)$, where θ_p is uniformly distributed over $[-\pi \pi]$. The CP is chosen long enough to accommodate the wireless channel delay spread.

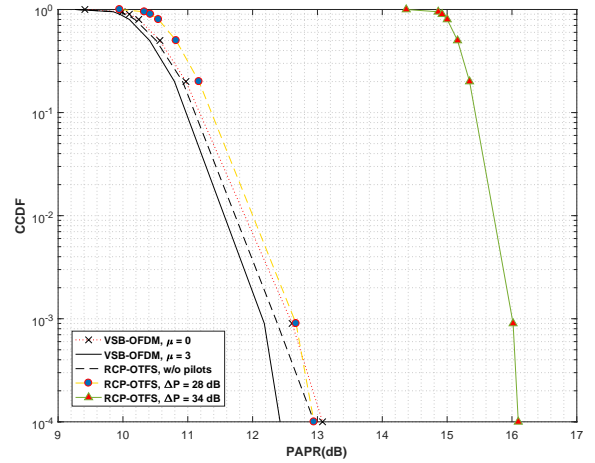


Fig. 3: CCDF of PAPR for OFDM and OTFS

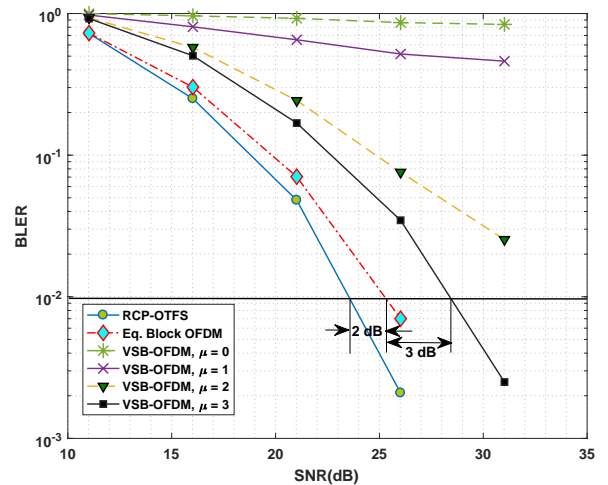


Fig. 4: BLER performance for 16QAM at 500kmph

We hypothesize that a large ΔP may have an effect on

PAPR of s (9). We present the CCDF of RCP-OTFS for $\Delta P = 34$ dB and $\Delta P = 28$ dB in Fig.3. It can be seen that at $\Delta P = 34$ dB, which arises when we let P_T same for VSB-OFDM and RCP-OTFS, PAPR of RCP-OTFS is nearly 3.5 dB higher. We therefore reduce ΔP so that PAPR may be reduced. We have found that for given configuration, if $\Delta P \leq 28$ dB, there is no further reduction in PAPR of RCP-OTFS signal s than that of OFDM, and that it is very close to that of VSB-OFDM. Therefore we have kept the $\Delta P = 28$ dB in the performance evaluation presented here. Further, reduction in ΔP implies that power of data RCP-OTFS is higher than that of VSB-OFDM by 0.154dB/symbol. Therefore, there is an additional gain in SNR for OTFS.

Figure 4 presents the performance of different waveforms for 16 QAM modulation at the vehicular speed of 500 kmph. It can be observed that performance of VSB-OFDM becomes better with increasing value of μ as expected and supported by literature. This is because the effect of Doppler spread reduces with increased sub-carrier bandwidth as post processing SNR for OFDM under Doppler, $\Gamma \propto (\frac{\Delta f}{\nu_{max}})^2$ [18]. It can also be observed that OTFS outperforms VSB-OFDM even with $\mu = 3$. For example at the BLER of 10^{-1} , OTFS has SNR gain of 3.5 dB over VSB-OFDM ($\mu = 3$). This gain further increases to nearly 5 dB at BLER of 10^{-2} . This result can be attributed to two reasons (i) OTFS has an interleaving gain and, (ii) OTFS uses ICI cancellation LMMSE receiver whereas VSB-OFDM uses a simple single-tap receiver. Further, at the BLER of 10^{-1} and 10^{-2} , OTFS has gain of 1 dB and 2 dB respectively over block OFDM. As it has been mentioned above that both Block OFDM and RCP-OTFS use FEC and LMMSE equalizer while the difference in transmitted signal is time interleaving as (Sec.II-B and shown in Fig.1), therefore it can be said that this gain is primarily due to the interleaving. We have observed similar results for other vehicular speeds as well for other modulation and chose to not include them here for brevity. Thus, it can be concluded that OTFS performs better than other contender waveforms in vehicular scenarios by virtue of its interleaving and LMMSE interference cancellation.

VI. CONCLUSIONS

In this work, we have detailed the signal generation of OTFS and explained how it could be viewed in an alternative form as block OFDM with time interleaving. We have identified the exact gain due to such interleaving that OTFS obtains over a non-interleaved block OFDM while using FEC and practical channel estimation in a high-speed environment as proposed by 3GPP. We found that the interleaving gain is up to 5 dB as compared to block OFDM and VSB-OFDM. We have also found that the SNR gain due to ICI cancellation, i.e., MMSE receiver, is about 3 dB when compared with the single-tap VSB receiver.

We have also described the pilot power allocation issue and its effect on PAPR. We found that the pilot power of OTFS can be made lower than OFDM and thus is less sensitive to channel estimation error. Further, the percentage resource used

for pilots in OTFS is less than OFDM, and hence spectral efficiency (SE) of OTFS is higher. Moreover, OTFS uses lower CP overhead than OFDM, which further increases the SE of OTFS. Finally, it can be said that OTFS has high SE, better resilience to ICI due to interference canceling receiver and interleaving, which is not usually available in an OFDM system.

REFERENCES

- [1] L. Liang, H. Peng, G. Y. Li, and X. Shen, "Vehicular Communications: A Physical Layer Perspective," *IEEE Transactions on Vehicular Technology*, vol. 66, no. 12, pp. 10647–10659, Dec. 2017.
- [2] R. Hadani, S. Rakib, M. Tsatsanis, A. Monk, A. J. Goldsmith, A. F. Molisch, and R. Calderbank, "Orthogonal Time Frequency Space Modulation," in *2017 IEEE Wireless Communications and Networking Conference (WCNC)*, Mar. 2017, pp. 1–6.
- [3] P. Raviteja, Y. Hong, E. Viterbo, and E. Biglieri, "Practical Pulse-Shaping Waveforms for Reduced-Cyclic-Prefix OTFS," *IEEE Transactions on Vehicular Technology*, vol. 68, no. 1, pp. 957–961, Jan. 2019.
- [4] P. Raviteja, E. Viterbo, and Y. Hong, "OTFS Performance on Static Multipath Channels," *IEEE Wireless Communications Letters*, pp. 1–1, 2019.
- [5] R. Hadani and A. Monk, "OTFS: A New Generation of Modulation Addressing the Challenges of 5g," *arXiv:1802.02623 [cs, math]*, Feb. 2018, arXiv: 1802.02623. [Online]. Available: <http://arxiv.org/abs/1802.02623>
- [6] S. Tiwari, S. S. Das, and V. Rangamgari, "Low complexity LMMSE receiver for OTFS," *IEEE Communications Letters*, pp. 1–1, 2019.
- [7] P. Raviteja, K. T. Phan, Y. Hong, and E. Viterbo, "Interference Cancellation and Iterative Detection for Orthogonal Time Frequency Space Modulation," *IEEE Transactions on Wireless Communications*, vol. 17, no. 10, pp. 6501–6515, Oct. 2018.
- [8] S. S. Das, E. D. Carvalho, and R. Prasad, "Variable sub-carrier bandwidth in OFDM framework," *Electronics Letters*, vol. 43, no. 1, pp. 46–47, Jan. 2007.
- [9] S. S. Das, E. De Carvalho, and R. Prasad, "Variable Sub-Carrier Bandwidths in OFDM Systems," in *2007 IEEE 65th Vehicular Technology Conference - VTC2007-Spring*, Apr. 2007, pp. 1866–1870, iSSN: 1550-2252.
- [10] S. Das, M. Rahman, and F. Fitzek, "Multi rate orthogonal frequency division multiplexing," in *IEEE International Conference on Communications, 2005. ICC 2005*, 2005, vol. 4, May 2005, pp. 2588–2592 Vol. 4, iSSN: 1550-3607, 1938-1883.
- [11] 3GPP, *NR Physical channels and modulation (Release 15)*, TS 38.211, V 15.2, 3GPP, 2018.
- [12] —, *Study on Channel Model for Frequencies from 0.5 to 100 GHz (Release 15)*, TR 38.901, V 15.0, 3GPP, 2018.
- [13] F. Wiffen, L. Sayer, M. Z. Bocus, A. Doufexi, and A. Nix, "Comparison of OTFS and OFDM in Ray Launched sub-6 GHz and mmWave Line-of-Sight Mobility Channels," in *2018 IEEE 29th Annual International Symposium on Personal, Indoor and Mobile Radio Communications (PIMRC)*, Sep. 2018, pp. 73–79, iSSN: 2166-9589, 2166-9570.
- [14] P. Raviteja, K. T. Phan, and Y. Hong, "Embedded Pilot-Aided Channel Estimation for OTFS in DelayDoppler Channels," *IEEE Transactions on Vehicular Technology*, vol. 68, no. 5, pp. 4906–4917, May 2019.
- [15] P. Raviteja, K. T. Phan, Y. Hong, and E. Viterbo, "Embedded Delay-Doppler Channel Estimation for Orthogonal Time Frequency Space Modulation," in *2018 IEEE 88th Vehicular Technology Conference (VTC-Fall)*, Aug. 2018, pp. 1–5.
- [16] Jianguang Zhao, F. Zarkeshvari, and A. H. Banihashemi, "On implementation of min-sum algorithm and its modifications for decoding low-density parity-check (ldpc) codes," *IEEE Transactions on Communications*, vol. 53, no. 4, pp. 549–554, April 2005.
- [17] M. J. Fernandez-Getino Garcia, J. M. Paez-Borrillo, and S. Zazo, "Dft-based channel estimation in 2d-pilot-symbol-aided ofdm wireless systems," in *IEEE VTS 53rd Vehicular Technology Conference, Spring 2001. Proceedings (Cat. No.01CH37202)*, vol. 2, May 2001, pp. 810–814 vol.2.
- [18] S. S. Das, E. D. Carvalho, and R. Prasad, "Performance Analysis of OFDM Systems with Adaptive Sub Carrier Bandwidth," *IEEE Transactions on Wireless Communications*, vol. 7, no. 4, pp. 1117–1122, Apr. 2008.